Sequence Preference of 7,12-Dimethylbenz[*a*]anthracene-*syn*-diol Epoxide−DNA Binding in the Mouse H-*ras* Gene Detected by UvrABC Nucleases†

James X. Chen,‡ Annie Pao,‡ Yi Zheng,‡ Xiancang Ye,‡ Alexander S. Kisleyou,§ Rebecca Morris,|| Thomas J. Slaga,‡ Ronald G. Harvey,§ and Moon-shong Tang*,‡

Department of Carcinogenesis, University of Texas M. D. Anderson Cancer Center, Science Park-Research Division, Smithville, Texas 78957, Lankenau Medical Research Center, 100 Lancaster Avenue West of City Line, Wynnewood, Pennsylvania 19096, and Ben May Institute, University of Chicago, Chicago, Illinois 60637

Received February 20, 1996; Revised Manuscript Received May 16, 1996⊗

ABSTRACT: We have found that 7,12-dimethylbenz[*a*]anthracene-*syn*-diol epoxide (*syn*-DMBADE)-modified DNA fragments are sensitive to UvrABC incision. The incisions occur mainly seven bases 5′ and four bases 3′ of a *syn*-DMBADE-modified adenine or guanine residue. The kinetics of UvrABC incision at different sequences in a DNA fragment are the same, and the extent of UvrABC incision is proportional to the *syn*-DMBADE concentration. On the basis of these results, we have concluded that UvrABC incision on *syn*-DMBADE−DNA adducts is independent of DNA sequence and is quantitative. Using the UvrABC incision method, we have analyzed the *syn*-DMBADE−DNA binding spectrum in several defined DNA fragments, including the first two exons of the mouse H-*ras* gene. We have found that both guanine and adenine residues in codons 12, 13, and 61 of the H-*ras* gene are strong *syn*-DMBADE binding sites. These results suggest that the initial binding of DMBADE may greatly contribute to the frequency of H-*ras* mutations. Results from dinucleotide binding analysis indicate that the 5′-nearest neighbor displays a greater effect on *syn*-DMBADE−DNA binding than the 3′-nearest neighbor.

7,12-Dimethylbenz[*a*]anthracene (DMBA)[1] is a potent carcinogen (Slaga et al., 1979; Bigger et al., 1983; Manam et al., 1992a). Metabolically activated *syn*- and *anti*-dihydrodiol epoxide forms of DMBA (Figure 1) are reactive with DNA (Bigger et al., 1980a,b; Cooper et al., 1980; Dipple et al., 1984; DiGiovanni et al., 1986), and the binding occurs mainly at guanine and adenine residues (Dipple et al., 1983; Moschel et al., 1983; Sawicki et al., 1983; Morse et al., 1987; Smolarek et al., 1987; Cheng et al., 1988; Verica et al., 1989). These DNA adducts have been extensively studied using various methods (Schmeiser et al., 1988; Yang et al., 1990; RamaKrishna et al., 1992) and have been ascribed as the initial lesions that trigger carcinogenesis (Quintanilla et al., 1986).

One distinct molecular characteristic associated with DMBA-initiated carcinogenesis is the oncogenic activation of the *ras* gene family caused by a point mutation in codon 12, 13, or 61 of the *ras* genes (Balmain & Brown, 1988; Barbacid, 1987; Bos, 1989; Sukumar, 1990; Manam et al., 1992b). Several laboratories have reported that more than 90% of the papillomas and squamous cell carcinomas induced in mice by the topical application of DMBA have point mutations in codon 61 of the H-*ras* gene (Bizub et al., 1986; Quintanilla et al., 1986, 1991; Gimenez-Conti et al., 1992; Robles et al., 1993). In contrast, the occurrence of mutations in codon 12 or 13 of the H-*ras* gene is rare in these skin tumors (Bizub et al., 1986; Quintanilla et al., 1986, 1991; Gimenez-Conti et al., 1992; Robles et al., 1993). Since all the guanine and adenine residues in codons 12, 13, and 61 can potentially form adducts with activated DMBA and mutations in any of these codons of the H-*ras* gene can potentially trigger carcinogenesis, one interesting and important question raised from these results is why most, if not all, DMBA-induced skin papillomas have a mutation in codon 61 but not in codon 12 or 13. It is possible that activated DMBADE may not efficiently form DNA adducts at codons 12 and 13, and/or the adducts formed in these sequences are repaired swiftly and efficiently. This important question motivated us to develop a method to detect DMBA−DNA adducts at the nucleotide sequence level.

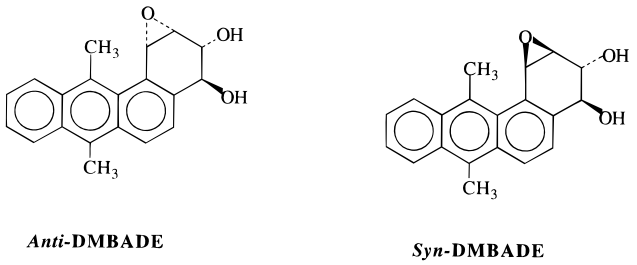

FIGURE 1: Chemical structure of *syn*- and *anti*-dihydrodiol epoxide forms of DMBA.

It has been well-established that the initial step of nucleotide excision repair in *Escherichia coli* is controlled by three gene products: UvrA, UvrB, and UvrC; these three proteins, working together (we term their collective functions as UvrABC nuclease), recognize and incise a variety of bulky chemical carcinogen−DNA adducts (Tang et al., 1988, 1992; Pierce et al., 1989, 1993; Kohn et al., 1992). We have

† This work was supported by Grant ES03124 from the United States Public Health Service and Grant 3955 from the Council for Tobacco Research-USA, Inc. J.X.C. is also supported by NIH Postdoctoral Training Grant CA09480.

* Corresponding author.
‡ University of Texas M. D. Anderson Cancer Center.
§ University of Chicago.
|| Lankenau Medical Research Center.

⊗ Abstract published in *Advance ACS Abstracts,* July 1, 1996.

[1] Abbreviations: DMBA 7,12-dimethylbenz[*a*]anthracene; *syn*-DMBADE, 7,12-dimethylbenz[*a*]anthracene-*syn*-diol epoxide; H-*ras*, Harvey-*ras*; BPDE, (±)-*r*-7,*t*-8-dihydroxy-9,10-epoxy-7,8,9,10-tetrahydrobenzo[*a*]pyrene; N-OH-AF, *N*-hydroxy-2-aminofluorene.

S0006-2960(96)00413-8 CCC: $12.00

previously found that UvrABC incises DNA adducts induced by benzo[*a*]pyrenediol epoxide (*anti* and *reverse* forms) specifically and quantitatively (Tang et al., 1992). In this report, we have quantified and characterized the mode of incision of UvrABC toward DNA modified with chemically synthesized *syn*-DMBADE. We have found that the UvrABC nuclease incises *syn*-DMBADE−DNA adducts quantitatively and specifically. Using this method, we have determined the *syn*-DMBADE binding spectrum in defined DNA sequences and, in particular, the mouse H-*ras*.

MATERIALS AND METHODS

Materials. Racemic *syn*-DMBADE was synthesized according to the method described previously (Lee & Harvey, 1986). BPDE and N-OH-AF were purchased from Chemsyn Science Laboratories. Restriction enzymes, T4 polynucleotide kinase, and DNA polymerase I (Klenow fragment) were obtained from New England BioLabs. Calf intestinal alkaline phosphatase was purchased from Promega. NACS Prepac convertible columns were purchased from BRL. All other chemicals and electrophoretic materials were obtained from either Sigma or Bio-Rad. [α-^{32}P]dCTP and [γ-^{32}P]-ATP (specific activity of approximately 3000 Ci/mmol) were purchased from DuPont New England Nuclear.

Restriction Fragment Isolation from Mouse and Human H-ras Genes and ^{32}P-End Labeling. The plasmid pUC8, containing an insert of exons 1 and 2 of the mouse H-*ras* gene at the *Pst*I site (Brown et al., 1988), was kindly supplied by Dr. Allan Balmain, Beatson Institute for Cancer Research, Glasgow, Scotland. The plasmid pBR322, containing an insert of exons 1 and 2 of the human H-*ras* oncogene at the *Bam*HI site, was obtained from American Type Tissue Culture Collection. These plasmids were purified by cesium chloride density gradient centrifugation. The 285 bp *Sty*I-*Hin*fI fragment containing exon 1 of the mouse H-*ras* gene, the 194 bp *Hin*fI-*Nhe*I fragment containing exon 2 of the mouse H-*ras* gene, and the 308 bp *Kpn*I-*Bgl*I fragment containing exon 2 of the human H-*ras* gene were prepared by digesting the plasmids with restriction enzymes and were then 5′-^{32}P-end-labeled as described previously (Pierce et al., 1989). The 194 bp *Hin*fI-*Nhe*I fragment of the mouse H-*ras* gene containing exon 2 was prepared by digesting the mouse H-*ras* plasmid with *Nhe*I and *Hin*dIII, and the fragment was labeled at the 3′ sites, digested with *Hin*fI, and purified as described (Pierce et al., 1989).

syn-DMBADE, BPDE, and N-OH-AF Modification of DNA. syn-DMBADE and BPDE were dissolved in dimethyl sulfoxide to a concentration of 1 mg/mL. ^{32}P-labeled DNA fragments were dissolved in 90 μL of TE buffer [10 mM Tris and 1 mM EDTA (pH 7.8)], mixed with 10 μL of different concentrations of chemicals, and incubated at 25 °C for 2 h. Unreacted *syn*-DMBADE or BPDE was removed by multiple phenol and diethyl ether extractions. The modified DNA was then ethanol precipitated, washed with 70% ethanol, and dried under vacuum.

N-OH-AF was dissolved in argon-purged absolute ethanol to a concentration of 1 mg/mL. DNA fragments were dissolved in 90 μL of buffer solution [10 mM sodium citrate (pH 5.5)], mixed with 10 μL of N-OH-AF solution, and incubated at 25 °C for 3 h. The unreacted N-OH-AF was removed by repeated phenol and diethyl ether extractions, and the DNA was ethanol precipitated, washed, and dried as described above.

Purification of UvrA, UvrB, and UvrC Proteins. The UvrA, UvrB, and UvrC proteins were isolated from the *E. coli* K12 strain CH296 carrying plasmids pUNC 45 (*uvrA*), pUNC21 (*uvrB*), or pDR3274 (*uvrC*) (Thomas et al., 1985). These plasmids and the CH296 strain were kindly provided by Dr. A. Sancar, University of North Carolina, Chapel Hill, NC. The UvrA and UvrC proteins were purified using phosphocellulose and single-stranded DNA cellulose columns. UvrB proteins were purified using DEAE-Biogel-A, phenylagarose, and Affigel-Blue columns. The details of the purification procedures were essentially the same as those described previously (Sancar & Rupp, 1983) except that the steps of protein precipitation by poly(ethyleneimine) and ammonium sulfate were eliminated and a continuous salt gradient replaced the step gradient to elute the proteins (Tang, 1996).

UvrABC Nuclease Reactions. The UvrABC nuclease reactions were carried out in a reaction mixture (25 μL) containing 50 mM Tris-HCl (pH 7.5), 0.1 mM EDTA, 10 mM $MgCl_2$, 1 mM ATP, 100 mM KCl, 1 mM dithiothreitol, 15 nM UvrA, 15 nM UvrB, 15 nM UvrC, and substrate DNA. The mixture was incubated at 37 °C for 1 h, and the reactions were stopped by phenol and diethyl ether extractions and followed by ethanol precipitation in the presence of aqueous ammonium acetate (2.5 M). The precipitated DNA was washed with 70% ethanol and dried under vacuum.

DNA Sequencing, Gel Electrophoresis, and Autoradiography. The single 5′ and 3′-^{32}P-end-labeled DNA fragments were sequenced by the chemical cleavage method (Maxam & Gilbert, 1980). The ^{32}P-labeled DNA fragments with or without UvrABC enzyme treatments were suspended in sequencing tracking dye (80% v/v deionized formamide, 0.1% xylene cyanol, and 0.1% bromophenol blue), and heated at 90 °C for 4 min, and the reaction was quenched in an ice bath. The samples were applied to a 0.4−0.8 mm denaturing sequencing gel consisting of 8% acrylamide and 7 M urea in TBE buffer [50 mM Tris-HCl, 50 mM borate, and 10 mM EDTA (pH 8.3)]. The gels were dried in a Bio-Rad gel dryer, initially exposed to a phosphor screen and then to a Kodak X-Omat RP film at −70 °C for various lengths of time. The intensity of bands was determined by a PhosphorImager (Molecular Dynamics).

RESULTS

syn-DMBADE−DNA Adducts Are Sensitive to UvrABC Incision. It has been well-established that the UvrABC nuclease incises a variety of types of DNA damage, including damage that destabilizes as well as damage that stabilizes the DNA helix (Tang et al., 1988, 1992; Pierce et al., 1989, 1993; Kohn et al., 1992). The hallmarks of the UvrABC incision to damaged DNA are its dual incisions; the enzyme incises six to eight bases 5′ and three to five bases 3′ of the damaged base(s). In order to test whether UvrABC nucleases are able to recognize and incise *syn*-DMBADE−DNA adducts, DNA fragments labeled with ^{32}P at a single 5′ or 3′ end were reacted with UvrABC under standard reaction conditions, and the results are shown in Figure 2. When *syn*-DMBADE-modified 5′-^{32}P-end-labeled DNA was used as the substrate, the UvrABC reaction generated bands which corresponded to Maxam−Gilbert purine reaction ladders, but these bands were seven nucleotides smaller (lane 4, Figure 2A), with exceptions at positions 39 and 60; the adenine

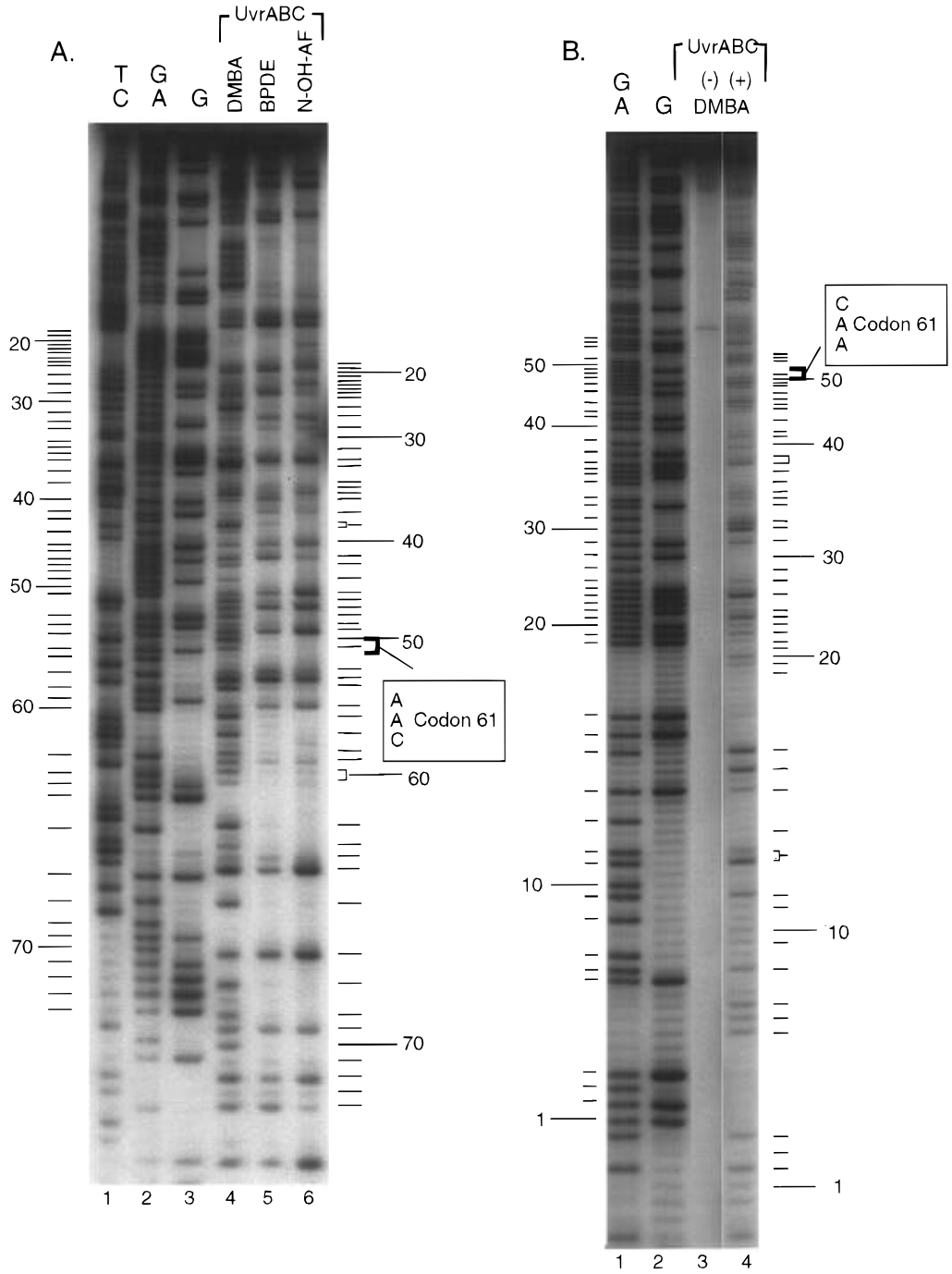

FIGURE 2: Typical autoradiograph of the electrophoretic separation of *syn*-DMBADE-modified DNA fragments after reaction with UvrABC nucleases. (A) 5′-^{32}P-end-labeled *Hin*fI-*Nhe*I 194 bp fragments of the mouse H-*ras* gene containing codon 61 were modified with 10^{-2} mg/mL *syn*-DMBADE (lane 4), 10^{-4} mg/mL BPDE (lane 5), or 10^{-1} mg/mL N-OH-AF (lane 6) and then reacted with UvrABC. (B) 3′-^{32}P-end-labeled *Hin*fI-*Nhe*I 194 bp fragments of the mouse H-*ras* gene were modified with (lane 4) and without (lane 3) *syn*-DMBADE (10^{-2} mg/mL) and then reacted with UvrABC. The carcinogen modifications, UvrABC nuclease reactions, and sequencing gel electrophoresis are described in the text. Lines on the left side of the panels represent the purine positions, and lines on the right side of the panels represent the corresponding UvrABC incision positions. Double lines represent the double-UvrABC incision positions on the 5′ or 3′ side of a modified purine. The UvrABC incision bands corresponding to codon 61 position are highlighted. G, GA, and TC are the Maxam−Gilbert sequencing reactions.

residues at each of these positions induced two UvrABC incision bands which were eight and seven nucleotides smaller than the corresponding Maxam−Gilbert bands.

When *syn*-DMBADE-modified 3′-^{32}P-end-labeled DNA was used as the substrate, the UvrABC reaction also generated bands which corresponded to Maxam−Gilbert purine reaction ladders, but these bands were four nucleotides smaller (lane 4 in Figure 2B), with exceptions at positions 13 and 39; the adenine residues at each of these positions induced two UvrABC cutting bands which were three and four nucleotides smaller than the corresponding Maxam−Gilbert bands. Since it has been shown that activated DMBA reacts with both adenine and guanine but not with pyrimidine residues (Bigger et al., 1983; Dipple et al., 1983; DiGiovanni et al., 1986; Mores et al., 1987; Smolarek et al., 1987; Cheng et al., 1988), we believe that these results show that UvrABC makes dual incisions seven bases 5′ and four bases 3′ of *syn*-DMBADE-modified purines. These results are consis-

tent with the published results which show that purified UvrABC typically makes dual incisions six to eight nucleotides 5′ and three to five nucleotides 3′ of a damaged base [for a review, see Van Houten (1990) and Sancar and Tang (1993)]. To typify these points, UvrABC was also reacted with the same DNA fragments which were modified with BPDE and N-OH-AF instead of DMBADE; Figure 2A shows that the UvrABC reactions generated bands corresponding only to guanine residues but seven nucleotides smaller. Since the adduction by BPDE and N-OH-AF modifications mainly occurs at guanine residues (Tang et al., 1982, 1992; Pierce et al., 1989), these results further support our interpretation that UvrABC incises both *syn*-DMBADE−adenine and −guanine adducts. It is worth noting that the relative intensities of the UvrABC incisions at the 5' and 3' sides of a *syn*-DMBADE-modified base are comparable; that is, a modified base which induces a strong 5' side UvrABC incision also induces a strong 3' side enzyme incision (see Figure 5A for a detailed comparison).

UvrABC Nucleases Incise syn-DMBADE−DNA Adducts Quantitatively, and the Incisions Are Sequence Independent. The intensities of *syn*-DMBADE-induced UvrABC incision bands shown in Figure 2 vary at different sequences; this could be due to different affinities of *syn*-DMBADE modification at different sequences or could be due to sequence dependent incision by UvrABC nucleases. Since no DNA polymerase or ligase is present in the UvrABC incision reaction, the incision must be an irreversible reaction (Van Houten, 1990; Sancar & Tang, 1993). It is therefore possible to distinguish between these two possibilities by kinetic analysis; that is, provided that the Uvr protein/substrate DNA ratio is larger than one, the kinetics of UvrABC incision at different sequences should reflect whether the DNA sequence plays a role in enzyme incision. The typical time course of UvrABC incision on the *syn*-DMBADE-modified DNA fragments is shown in Figure 3A (lanes 6−10); the intensity of cutting bands reaches a plateau after 20 min of incubation. In contrast, no UvrABC cutting was observed in unmodified DNA fragments (lanes 1−5 in Figure 3A). The slight reduction in the intensities of the UvrABC cutting bands after 60 min of incubation is probably due to the effect of nonspecific nuclease contamination in the Uvr proteins. A total of 20 bands in a well-separated region were chosen for quantification. The results shown in Figure 3B demonstrate that UvrABC incises DNA adducts formed in these sequences with identical kinetics and the incision reaches a plateau after 20 min of incubation. Since the molar ratio of UvrABC/DNA is 4.3 in these reaction conditions, these results strongly suggest that DNA sequence does not play a significant role in determining the efficiency of UvrABC incision. To further support this conclusion, we determined the efficiency of UvrABC incision at these sequences in DNA fragments modified with different concentrations of *syn*-DMBADE (lanes 14−18 in Figure 3A). Bands in the well-separated region were quantified, and the results of UvrABC incision versus *syn*-DMBADE concentration for different sequences were plotted in Figure 3C; the slopes for different sequences are not only linear but also about equal. Together, these results demonstrate that under our standard reaction conditions UvrABC nucleases quantitatively incise *syn*-DMBADE−DNA adducts.

syn-DMBADE−DNA Binding Spectrum in the Mouse H-ras Gene. Having established that under our standard reaction conditions UvrABC is able to incise *syn*-DMBADE-DNA adducts quantitatively, we then determined the DNA binding spectrum of this chemical in DNA fragments encompassing exon 1 (Figure 4) and exon 2 (Figure 2) of the mouse H-*ras* gene. The mouse H-*ras* gene was chosen because of the intriguing findings about the gene and the codon specificity of the mutations observed in papillomas induced by DMBA; there is ample evidence which demonstrates that more than 90% of the DMBA-induced papillomas in mouse skin have a mutation exclusively in codon 61 of the H-*ras* gene (Bizub et al., 1986; Quintanilla et al., 1986, 1991; Gimenez-Conti et al., 1992; Robles et al., 1993). These results indicate not only that DMBA may form DNA adducts at this sequence but also that it is possible that the purines in this codon have an intrinsically high affinity for DMBADE binding. It is therefore of interest to determine whether the UvrABC incision analysis can directly demonstrate this binding.

The typical autoradiographs are shown in Figures 2 and 4, and the quantitations are shown in Figure 5. These results demonstrate that every adenine, including the two in codon 61, and every guanine, including those in codons 12 and 13, in these sequences bind to *syn*-DMBADE. However, the degree of binding varies at different sequences. *syn*-DMBADE binds more strongly to the second adenine than to the first adenine in the codon 61 CAA sequence (lane 4 in Figure 2A); quantitatively, *syn*-DMBADE binds to the latter with an average affinity (Figure 5A). In contrast, *syn*-DMBADE binds to guanines in codons 12 and 13 with significantly higher than average affinities (Figure 5B).

Effect of Flanking Bases on syn-DMBADE−DNA Binding. It has been shown that the sequence context may influence the efficiency of chemical−DNA binding and photoproduct formation. In particular, the nearest neighbor bases greatly affect DNA alkylation by certain agents, such as mitomycin C, tomaymycin, and anthramycin (Kohn et al., 1992; Pierce et al., 1993). In order to determine the sequence effect on *syn*-DMBADE−DNA adduct formation, we analyzed two more DNA fragments: the 5′-^{32}P-end-labeled *Nhe*I-*Hin*fI fragment of exon 2 of mouse H-*ras* and the *Kpn*I-*Sma*I fragment of exon 2 of human H-*ras*. These DNA fragments were modified with different concentrations of *syn*-DMBADE, reacted with UvrABC nucleases, and separated by gel electrophoresis as described above. The binding spectra are shown in panels C and D of Figure 5.

Since the 5′TG*G sequence appears in all five of these fragments with high frequency and, furthermore, the intensities of the UvrABC incision band at this sequence among all five DNA fragments are relatively constant, for the purpose of comparison, all the other UvrABC incision band intensities were normalized to the intensity of the 5′TG*G sequence. To determine the effect of the 5′-nearest neighbor base on *syn*-DMBADE−DNA binding, the results were categorized according to 5′NuG* and 5′NuA*, where Nu represents any of the four nucleotides and A* and G* represent *syn*-DMBADE-bound adenines and guanines, respectively. The results in Table 1 demonstrate that the effect of the 5′ base on *syn*-DMBADE−DNA binding is dependent upon whether it is an adenine or guanine adduct; the preferred order of the base on the 5′ side for adenine adduct formation is C > A > T and G, and for guanine adduct formation, the order is T, A, and C > G.

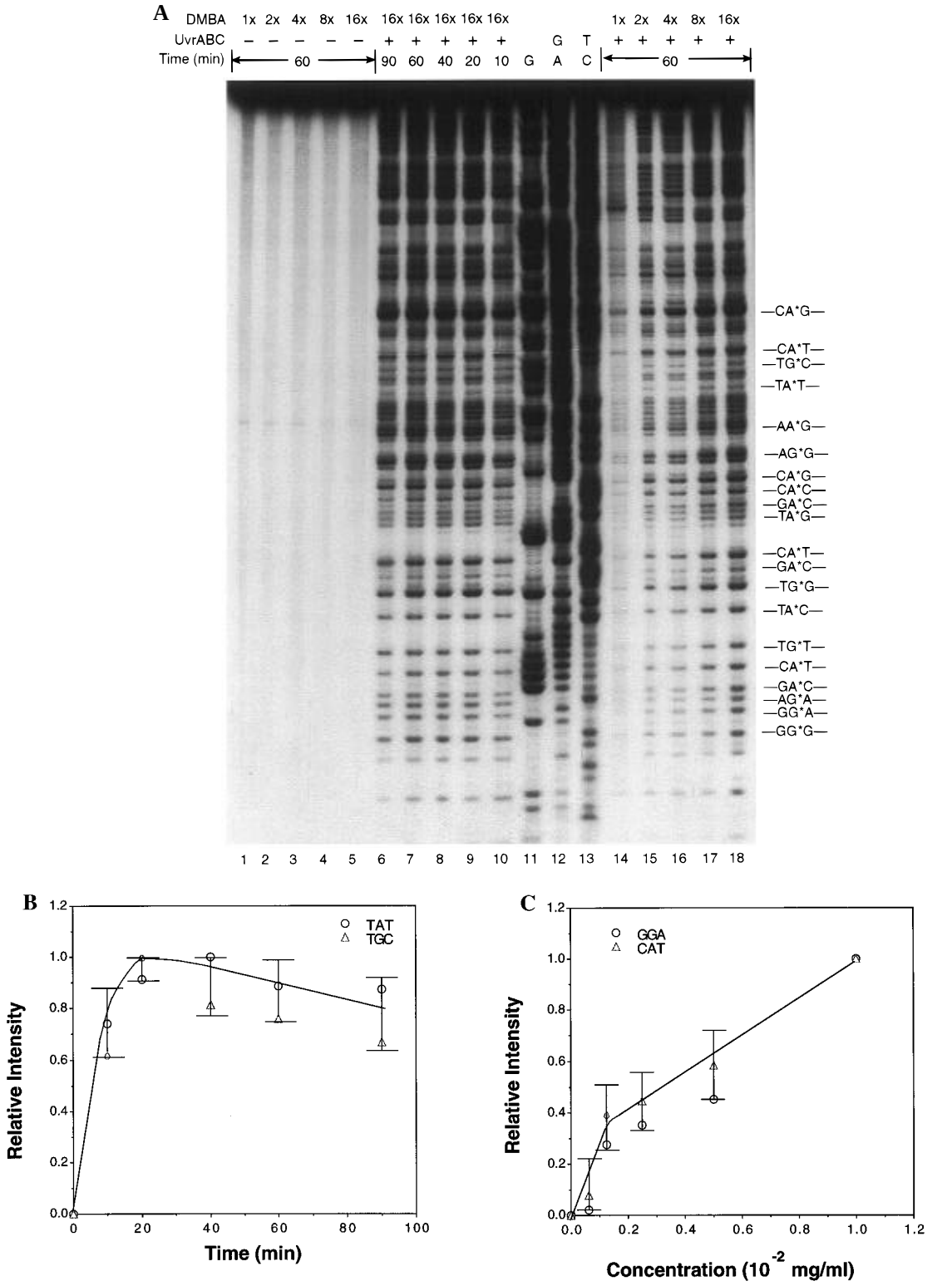

FIGURE 3: Time course of UvrABC incision on *syn*-DMBADE-modified DNA fragments and the effect of *syn*-DMBADE concentration on the UvrABC incision. (A) Autoradiograph. 5′-^{32}P-end-labeled *Hin*fI-*Nhe*I 194 bp fragments (0.45 pmol) of the mouse H-*ras* gene were modified with different concentrations of *syn*-DMBADE (1x represents 6.25×10^{-4} mg/mL *syn*-DMBADE) in a final volume of 100 μL. One-fifth of the modified DNA fragments (0.09 pmol) was then incubated with (+) or without (−) UvrABC nucleases for different periods of time, and the resulting DNAs were separated in an 8% sequencing gel as described in Figure 2. The trinucleotide nucleotide sequences (with * representing the *syn*-DMBADE modification site) which correspond to the UvrABC incision bands are depicted on the right side of the panel. The intensity of each UvrABC incision band was quantified in a PhosphorImager. (B) The time course of UvrABC incisions at different sequences on DNA fragments modified with 10^{-2} mg/mL *syn*-DMBADE (lanes 6−10). (C) The effect of *syn*-DMBADE concentration on the UvrABC incision at different sequences (lanes 14−18). The intensities of UvrABC cutting bands at different sequences on DNA fragments with different incubation times (lanes 6−10) or modified with different concentrations of *syn*-DMBADE (lanes 14−18) were normalized to the highest intensity of UvrABC cutting bands among the same sequences. The lines in panels B and C represent the mean value of the different sequences. For clarity, only two sequence points are presented in panels B and C; the rest of the sequence points (total of 20) are within the length of the bar.

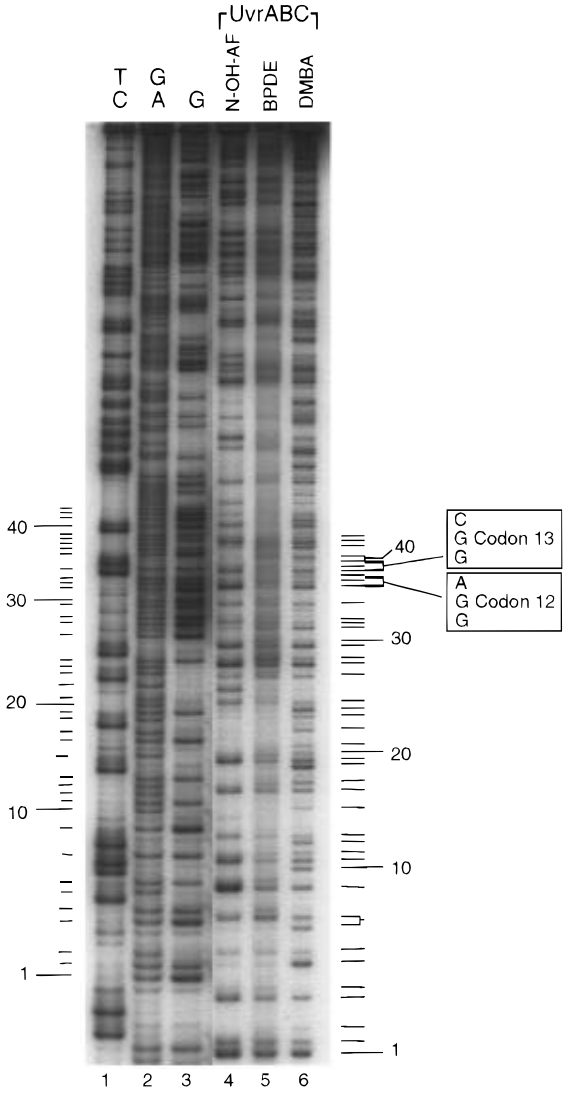

FIGURE 4: UvrABC incisions on the *syn*-DMBADE−DNA adducts formed at the mouse H-*ras* gene containing codons 12 and 13. 5′-^{32}P-end-labeled *Sty*I-*Hin*fI 285 bp fragments (0.45 pmol) of the H-*ras* gene were modified with *syn*-DMBADE (10^{-2} mg/mL, lane 6), BPDE (10^{-4} mg/mL, lane 5), or N-OH-AF (10^{-1} mg/mL, lane 4). One-fifth of the modified DNA fragments (0.09 pmol) was reacted with UvrABC and then separated in a sequencing gel using the same method as described in Figure 2. Lines on the left side of the panel represent the purine positions, and lines on the right side of the panel represent the corresponding UvrABC incision positions. The UvrABC incision bands corresponding to codons 12 and 13 are highlighted. G, GA, and TC are Maxam−Gilbert sequencing reactions.

To determine the effect of the 3′-nearest neighbor base on *syn*-DMBADE−DNA binding, the results were categorized according to 5′A*Nu′ and 5′G*Nu′. The results indicate that the effect of the 3′-nearest neighbor base on the efficiency of *syn*-DMBADE−DNA adduct formation is not as significant as the effect of the 5′-nearest neighbor base; in fact, the differences among different bases on the 3′-neighbor are statistically insignificant.

The data base obtained from the five DNA fragments also allowed us to analyze the *syn*-DMBADE−DNA binding affinity among the 16 trinucleotide combinations (Table 2). It appears that the *syn*-DMBADE−DNA binding in different trinucleotides can be grouped into three categories: strong, medium, and weak. For *syn*-DMBADE−adenine adduct formation, CAG and CAC are the optimal sequences, followed by CAT, AAT, TAC, AAG, CAA, GAA, AAC, TAA, GAC, TAG, TAT, and GAG; AAA and GAT are the weak sequences for adduct formation. For *syn*-DMBADE−guanine adduct formation, TGG is the optimal sequence, followed by CGC, AGA, AGG, AGT, and TGT and then by CGG, CGT, TGA, GGT, GGG, CGA, AGC, and GGA; TGC and GGC are the weak sequences for adduct formation.

DISCUSSION

We have previously successfully used UvrABC nucleases isolated from *E. coli* cells to detect DNA adducts induced by the bulky chemical carcinogens *N*-acetoxy-2-acetylaminofluorene, N-OH-AF, and BPDE (*anti* and *reverse* forms) and the antitumor antibiotics anthramycin, tomaymycin, and mitomycin C at the sequence level (Tang et al., 1988, 1992; Pierce et al., 1989, 1993; Kohn et al., 1992). In this study, we present evidence to demonstrate that UvrABC also cuts *syn*-DMBADE adducts specifically and quantitatively, and the mode of incision is similar to the enzyme cutting of other kinds of DNA adducts, thus allowing us to use this method to determine the DNA binding specificity of this chemical. Although both *syn*-DMBADE−DNA and *anti*-DMBADE−DNA are the major metabolic products responsible for binding to DNA (Dipple et al., 1984; DiGiovanni et al., 1986), *anti*-DMBADE was not included in the present study because of its extremely unstable nature. Nonetheless, we did find that *syn*-DMBADE appears to be a potent agent in inducing papillomas in mouse skin using the two-stage tumorigenesis protocol (preliminary results). Therefore, information on *syn*-DMBADE−DNA binding is important for understanding DMBA-induced tumorigenesis.

Our results show that purines in codons 12, 13, and 61 of the mouse H-*ras* gene are *syn*-DMBADE−DNA binding sites; these results suggest that the mutations observed in DMBA-treated mice may originate from adduct formation in these sequences. The majority of the mutations observed in the mouse skin papillomas induced by DMBA occur at the first adenine residue of codon 61 (Bizub et al., 1986; Quintanilla et al., 1986, 1991; Gimenez-Conti et al., 1992; Robles et al., 1993). Surprisingly, however, we found that this base has only a slightly above average *syn*-DMBADE binding affinity. In contrast, guanine residues in codons 12 and 13, in which mutations are rarely observed in mouse skin papillomas induced by DMBA (Bizub et al., 1986; Quintanilla et al., 1986, 1991; Gimenez-Conti et al., 1992; Robles et al., 1993), have a strong affinity for *syn*-DMBADE binding. These results raise three possibilities to account for the high incidence of DMBA-induced mutations at the first adenine of codon 61 of the H-*ras* gene in mouse skin. (1) *In vivo*, activated DMBA binds preferentially to the first adenine of codon 61 of H-*ras*. (2) *In vivo*, the DMBADE−DNA adducts formed at the first adenine of codon 61 of H-*ras* are not repaired efficiently. (3) *In vivo*, a DMBADE−adenine adduct is more likely to result in a mutation than a DMBADE−guanine adduct. It is conceivable that the efficiency of DMBADE−DNA binding depends not only on the primary DNA sequence but also on factors such as chromatin structure, nucleosome and other protein association, and transcriptional activity. Using the ligation-mediated PCR method, Tornaletti and Pfeifer (1994) and Gao et al. (1994) found that cyclobutane pyrimidine dimer repair is sequence dependent, and using a similar method, Wei et al. (1995) recently found that the mutation hot spots in the

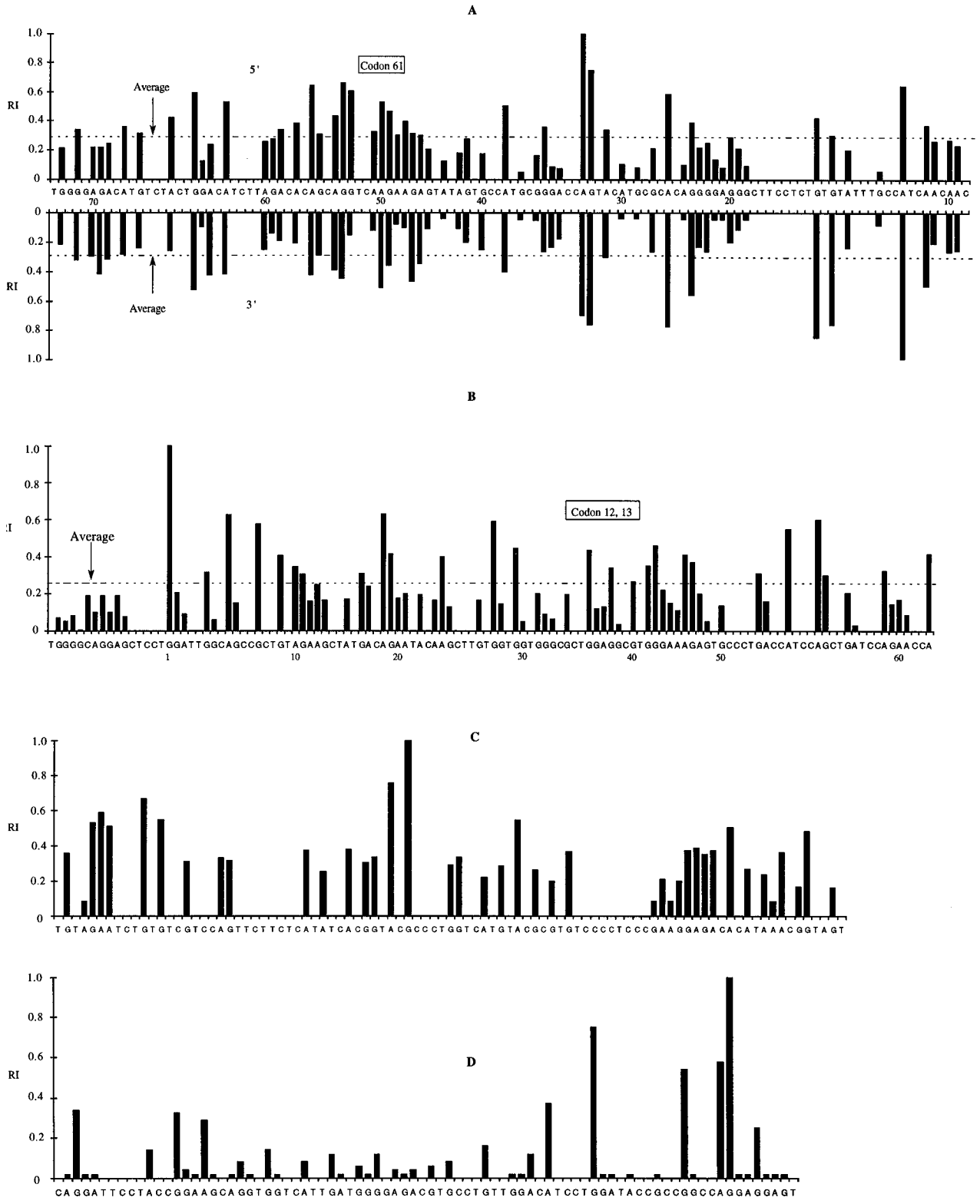

FIGURE 5: *syn*-DMBADE−DNA binding spectrum in (A) the 194 bp *Nhe*I-*Hin*fI fragment of the coding strand of exon 2 in the mouse H-*ras* gene, (B) the 285 bp *Sty*I-*Hin*fI fragment of the coding strand of exon 1 in the mouse H-*ras* gene, (C) the 194 bp *Nhe*I-*Hin*fI fragment of the noncoding strand of exon 2 in the mouse H-*ras* gene, and (D) the 308 bp *Kpn*I-*Sma*I fragment of the coding strand of exon 2 in the human H-*ras* gene. These DNA fragments were single-end labeled with ^{32}P, modified with *syn*-DMBADE, reacted with UvrABC nucleases, and then separated by gel electrophoresis, as described in Figure 2. The intensities of UvrABC incision bands in well-separated regions were quantified in a PhosphorImager. The extent of *syn*-DMBADE−DNA binding is represented by the relative intensity (RI) of UvrABC incision bands. The RI was calculated on the basis of RI = I_i/I_{max}, where I_i is the intensity of each UvrABC incision band and I_{max} is the UvrABC incision band with the highest intensity in an autoradiograph. In panel A, the results in the upper panel are obtained from 5′-^{32}P-end-labeled fragments, and the results in the lower panel are obtained from 3′-^{32}P-end-labeled DNA fragments, as shown in Figures 2 and 4, respectively. The height of the dotted lines represents the average RI.

human hypoxanthine phosphoribosyltransferase gene correspond with the repair "cold spots". These events exemplify the importance of determining DNA damage at the sequence level in order to understand its biological consequences. It

Table 1: Relative Intensities (RIs) Observed for the 5′ Base (Nu) and 3′ Base (Nu′) Flanking the *syn*-DMBADE−Guanine or −Adenine Modification Sites

5′ base (NuG* or NuA*)	no. of sites	normalized relative intensity[a]	3′ base (G*Nu′ or A*Nu′)	no. of sites	normalized relative intensity[a]
TG*	38	74 ± 15	G*G	40	73 ± 23
AG*	35	71 ± 13	G*T	33	68 ± 16
CG*	17	66 ± 13	G*A	36	51 ± 15
GG*	42	38 ± 11	G*C	23	44 ± 7
CA*	34	87 ± 9	A*G	36	66 ± 17
AA*	16	63 ± 9	A*C	27	66 ± 23
TA*	20	53 ± 10	A*A	17	52 ± 6
GA*	36	38 ± 6	A*T	26	51 ± 10

[a] The relative intensities were calculated from the PhosphorImager data obtained from the UvrABC nuclease treated 5′- or 3′-end-labeled DNA fragments of the *ras* gene described in Figure 4. The numbers are normalized relative intensities observed by using 5′TG*G as the "standard unit", and the ± value represents "standard error".

Table 2: Relative Intensities (RIs) Observed for the *syn*-DMBADE Trinucleotide Binding Sites 5′NuG*Nu′ and 5′NuA*Nu′

sequence 5′NuG*Nu′	no. of sites	normalized RI[a]	sequence 5′NuA*Nu′	no. of sites	normalized RI[a]
TG*G	13	100 ± 26	CA*G	12	100 ± 9
CG*C	6	82 ± 18	CA*C	7	91 ± 8
AG*A	12	79 ± 14	CA*T	11	79 ± 8
AG*G	9	79 ± 11	AA*T	2	78 ± 8
AG*T	7	79 ± 27	TA*C	7	75 ± 33
TG*T	13	76 ± 17	AA*G	8	75 ± 21
CG*G	5	63 ± 9	CA*A	4	61 ± 9
CG*T	4	59 ± 15	GA*A	9	56 ± 9
TG*A	6	55 ± 22	AA*C	4	52 ± 12
GG*T	9	53 ± 24	TA*A	2	51 ± 4
GG*G	13	45 ± 24	GA*C	9	47 ± 10
CG*A	2	44 ± 22	TA*G	5	41 ± 11
AG*C	7	43 ± 15	TA*T	6	41 ± 8
GG*A	16	29 ± 11	GA*G	11	35 ± 8
TG*C	6	26 ± 11	AA*A	2	21 ± 3
GG*C	4	18 ± 3	GA*T	7	10 ± 2

[a] The relative intensities were calculated by the same method as in Table 1.

is therefore crucial to determine the formation and repair of DMBADE−DNA adducts at the sequence level for understanding the gene-specific and sequence-specific activation of *ras* and factors which affect these processes. The specificity of UvrABC incision on this DNA adduct provides us with a useful tool to determine the binding sites *in vivo* and to investigate the effects of these factors.

It is worth noting that high-performance liquid chromatography analysis of DNA isolated from skin cells of DMBA-treated mice identified both adenine and guanine *anti*-DMBADE peaks, and only one major *syn*-DMBADE−adenine adduct and one minor *syn*-DMBADE−guanine adduct have been identified (Cheng et al., 1988; Yang et al., 1990; Schmeiser et al., 1988; RamaKrishna et al., 1992). In contrast UvrABC incision analysis identifies both adenine and guanine adducts from DNA fragments modified with *syn*-DMBADE *in vitro*; the ratio of adenine and guanine adducts is 1.25 on the basis of the calculation of the ratio of average relative intensity of UvrABC incision bands at these two adducts. Cheng et al. (1988) have shown that synthetic racemic *syn*-DMBADE reacts with deoxyadenylic acids and deoxyguanylic acids. It is possible that the low level of guanine−*syn*-DMBADE adducts detected in skin cells of DMBA-treated mice is due to different amounts of enantiomers of *syn*-DMBADE formed in the cellular system.

Results from Tables 1 and 2 suggest that the nearest neighbor bases may affect the efficiency of *syn*-DMBADE−DNA adduct formation, and this effect, to a certain degree, is also dependent upon whether it is an adenine or guanine adduction. *syn*-DMBADE is a plain and relatively small molecule, and its DNA binding is therefore probably determined by the electrostatic status of individual bases and the effect from base stacking. The binding affinity in trinucleotide binding for most cases is consistent with this dinucleotide analysis. However, there are some notable exceptions; for example, TG*C has a lower binding affinity than expected from dinucleotide analysis. On the other hand, CG*C has a higher binding affinity than expected from dinucleotide analysis. These results indicate that factors other than the nearest neighbor effect may also govern *syn*-DMBADE−DNA binding.

ACKNOWLEDGMENT

We thank Ms. Yen-Yee Tang for the critical review of the manuscript.

REFERENCES

Balmain, A., & Brown, K. (1988) *Adv. Cancer Res. 51,* 147−182.
Barbacid, M. (1987) *Annu. Rev. Biochem. 56,* 779−827.
Bigger, C. A. H., Tomaszewski, J. E., & Dipple, A. (1980a) *Carcinogenesis 1,* 15−20.
Bigger, C. A. H., Tomaszewski, J. E., Dipple, A., & Lake, R. S. (1980b) *Science 209,* 503−505.
Bigger, C. A. H., Sawicki, J. T., Blake, D. M., Raymond, L. G., & Dipple, A. (1983) *Cancer Res. 43,* 5647−5651.
Bizub, D., Wood, A. W., & Skalka, A. M. (1986) *Proc. Natl. Acad. Sci. U.S.A. 83,* 6048−6052.
Bos, J. L. (1989) *Cancer Res. 49,* 4682−4689.
Brown, K., Bailleul, B., Ramsden, M., Fee, F., Krumlau, R., & Balmain, A. (1988) *Mol. Carcinog. 1,* 161−170.
Cheng, S. C., Prakash, A. S., Pigott, M. A., Hilton, B. D., Lee, H., Harvey, R. G., & Dipple, A. (1988) *Carcinogenesis 9,* 1721−1723.
Cooper, C. S., Ribeiro, O., Hewer, A., Walsh, C., Grover, P. L., & Sims, P. (1980) *Chem.−Biol. Interact. 29,* 357−367.
DiGiovanni, J., Fisher, E. P., & Sawyer, T. W. (1986) *Cancer Res. 46,* 4400−4405.
Dipple, A., Piggott, M., Moschel, R. C., & Costantino, N. (1983) *Cancer Res. 43,* 4132−4135.
Dipple, A., Pigott, M. A., Bigger, C. A. H., & Blake, D. M. (1984) *Carcinogenesis 5,* 1087−1090.
Gao, S., Drouin, R., & Holmquist, G. P. (1994) *Science 263,* 1438−1440.
Gimenez-Conti, I. B., Sharon, A. B., Stockman, S. L., Conti, C. J., & Slaga, T. J. (1992) *Mol. Carcinog. 5,* 259−263.
Kohn, H., Li, V.-S., & Tang, M.-s. (1992) *J. Am. Chem. Soc. 114,* 5501−5509.
Lee, H., & Harvey, R. G. (1986) *J. Org. Chem. 51,* 3502−3507.
Manam, S., Storer, R. D., Prahalada, S., Leander, K. R., Kraynak, A. R., Ledwith, B. J., van Zwieten, M. J., Bradley, M. O., & Nichols, W. W. (1992a) *Cancer Res. 52,* 3347−3362.
Manam, S., Store, R. D., Prahalada, S., Leander, K. R., Kraynak, A. R., Hammermeister, C. L., Joslyn, D. J., Ledwith, B. J., Zweiten, M. J., Bradley, M. O., & Nichols, W. W. (1992b) *Mol. Carcinog. 6,* 68−75.
Maxam, A. M., & Gilbert, W. (1980) *Methods Enzymol. 65,* 499.
Morse, M. A., Baird, W. M., & Carlson, G. P. (1987) *Cancer Res. 47,* 4571−4575.
Moschel, R. C., Pigott, M. A., Costantino, N., & Dipple, A. (1983) *Carcinogenesis 4,* 1201−1204.
Pierce, J. R., Case, R., & Tang, M.-s. (1989) *Biochemistry 28,* 5821−5826.
Pierce, J. R., Nazimiec, M., & Tang, M.-s. (1993) *Biochemistry 32,* 7069−7078.

Quintanilla, M., Brown, K., Ramsden, M., & Balmain, A. (1986) *Nature 322,* 78−80.
Quintanilla, M., Haddow, S., Jonas, D., Jaffe, D., Bowden, G.-T., & Balmain, A. (1991) *Carcinogenesis 12,* 1875−1881.
RamaKrishna, N. V. S., Devanesan, P. D., Rogan, E. G., Cavalieri, E. L., Jeong, H., Jankowiak, R., & Small, G. J. (1992) *Chem. Res. Toxicol. 5,* 220−226.
Robles, A. I., Gimenez-Conti, I. B., Roop, D., Slaga, T. J., & Conti, C. J. (1993) *Mol. Carcinog. 7,* 94−98.
Sancar, A., & Rupp, W. D. (1983) *Cell 32,* 249−260.
Sancar, A., & Tang, M.-s. (1993) *Photochem. Photobiol. 57,* 905−921.
Sawicki, J. T., Moschel, R., & Dipple, A. (1983) *Cancer Res. 43,* 3212−3218.
Schmeiser, H., Dipple, A., Schurdak, M. E., Randerath, E., & Randerath, K. (1988) *Carcinogenesis 9,* 633−638.
Slaga, T. J., Gleaso, G. H., DiGiovanni, J., Sukumaran, K. B., & Harvey, R. G. (1979) *Cancer Res. 39,* 1934−1936.
Smolarek, T. A., Baird, W. M., Fisher, E. P., & DiGiovanni, J. (1987) *Cancer Res. 47,* 3701−3706.
Sukumar, S. (1990) *Cancer Cell 2,* 199−204.
Tang, M.-s. (1996) in *Technologies for Detection of DNA Damage and Mutations* (Pferfer, G., Ed.) Plenum Publishing Corporation (in press).
Tang, M.-s., Lieberman, M. W., & King, C. M. (1982) *Nature 299,* 646−648.
Tang, M.-s., Lee, C.-S., Doisy, R., Ross, L., Needham-Van-Devanter, D. R., & Hurley, L. H. (1988) *Biochemistry 27,* 893−901.
Tang, M.-s., Pierce, J. R., Doisy, R. P., Nazimiec, M. E., & MacLeod, M. C. (1992) *Biochemistry 31,* 8429.
Thomas, D. C., Levy, M., & Sancar, A. (1985) *J. Biol. Chem. 260,* 9875−9883.
Tornaletti, S., & Pfeifer, G. P. (1994) *Science 263,* 1436−1438.
Van Houten, B. (1990) *Microbiol. Rev. 54,* 18−51.
Verica, J. A., Cheng, S. C., & Dipple, A. (1989) *Carcinogenesis 10,* 567−570.
Wei, D., Maher, V. M., & McCormick, J. J. (1995) *Proc. Natl. Acad. Sci. U.S.A. 92,* 2204−2208.
Yang, P. F., & Randerath, K. (1990) *Carcinogenesis 11,* 159−164.

BI9604136